

Magnetism in diamond graphene nanoflakes

Phung Thi Thu^{1,2,*}, Nguyen Thi Mai³, Pham Thi Lien³, Nguyen Thanh Tung³

¹Graduate University of Science and Technology, Vietnam Academy of Science and Technology,
18 Hoang Quoc Viet, Cau Giay, Ha Noi, Viet Nam

²University of Science and Technology of Hanoi, Vietnam Academy of Science and Technology,
18 Hoang Quoc Viet, Cau Giay, Ha Noi, Viet Nam

³Institute of Materials Science, Vietnam Academy of Science and Technology, 18 Hoang Quoc Viet,
Cau Giay, Ha Noi, Viet Nam

*Emails: thuphungi2@gmail.com

Received: 11 September 2021; Accepted for publication: 9 September 2022

Abstract. We numerically study in this work the magnetic properties induced by the on-site electron-electron interaction in graphene nanoflakes shaped diamond with a variety of sizes. By the mean-field Hubbard approximation, a phase transition in analogy to infinite graphene from non-magnetism to antiferromagnetism is observed. A very weak interaction U , approximately zero, is reported to be able to trigger magnetic ordering in a finite nanoflake compared to infinite structure. Furthermore, the investigation also indicates the edge and size dependence of magnetism. The antiferromagnetic ground state is of robust stability to larger zigzag nanoflake size and stronger interaction. The phase transition point, U_c , is found to be sensitive to the size denoted by means of the reduction of U_c as the size increases. The important role of edge effect causing the spin polarization along zigzag termination is confirmed for the diamond nanoflakes.

Keywords: Graphene nanoflakes, magnetism, phase transition point, mean-field Hubbard approximation.

Classification numbers: 2.2.1, 4.1.1, 4.10.4

1. INTRODUCTION

With the aim to exploit the spin degree freedom of electrons as an information factor for data storage and logic devices, spintronics has attracted much attention. Unlike the conventional electronic devices, spintronic devices consume a lower energy and have a faster processing speed. The spintronics effect is thus promoted to be one of the most promising technologies for further development of high-speed, low-energy consuming and multi-functional electronic nanodevices in the future [1]. In this regard, two-dimensional materials are considered as an excellent candidate to create ideal next-generation spintronic devices owing to interesting intrinsic physical phenomena, for example quantum spin Hall effect, long spin relaxation time, long spin diffusion length, etc. [2]. Among the outstanding 2D materials is nanostructured graphene.

The successful isolation of graphene not only breaks the limitation in Mermin-Wagner theorem, but paves also the way for a novel era, Graphene era, along with technological advancement. Thanks to unique electronic band structure near Fermi energy, pseudospin conservation, high thermal conductivity and electron mobility, biocompatibility, non-toxicity, etc. [3 - 5], graphene, typically graphene with nanostructure, has been widely distributed in most fields of research, moving from laboratory to practical applications in industry and human living. In the spintronic field, graphene possesses a weak spin-orbit coupling, resulting in the relatively easy control of the electron spin [6] by the external fields such as the electric field or the Rashba spin-orbit coupling. Many recent experimental results have confirmed the potential of graphene for spin transport with long spin diffusion lengths over tens of micrometers and long spin relaxation time at room temperature [7 - 9].

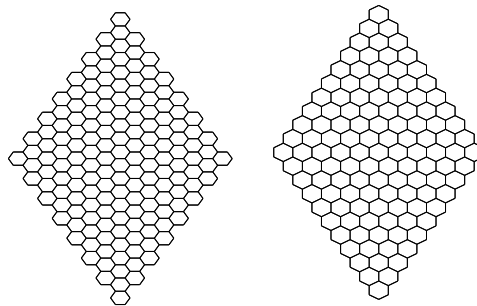


Figure 1. Diamond shaped graphene nanoflakes studied in this work with (left) armchair edge and (right) zigzag edge.

Most notably, finite sized graphene behaves as a new magnetic material with nontrivial magnetic properties. Consequently, the investigation of intrinsic magnetic properties in graphene has been highly encouraged as the main subject in many works. As indicated, infinite graphene is of non-magnetic material because of the balance of the two graphene sublattices. Yet numerous studies on both theory and experiment show that the magnetic ordering can be induced by defects such as vacancies, impurities effect, light and heavy adatoms, non-metal doping or Coulomb correlation because they are considered as sources so as to generate the imbalance in the two graphene sublattices [10 - 14]. On the other hand, the electronic states localized at zigzag edges and the reduction of dimensionality not only give rise to a significant modification in the electronic band structure, but also directly affect the magnetism at nanoscales. Theoretical and recent experimental findings have indicated the spin polarization on the zigzag graphene nanoribbons [4, 15]. The edge magnetism in other nanostructures has been theoretically predicted as well [16]. However, the issue concerning the intrinsic magnetism in graphene nanoflakes is still being debated due to the lack of experimental evidences.

Therefore, we focus on investigating systematically the on-site electron-electron interaction, denoted by Coulomb energy U , induced edge magnetism in diamond-shaped graphene nanoflakes with various sizes and two different edges; armchair and zigzag, using the mean-field Hubbard model at half-filling and zero temperature (Figure 1). According to the computational results, the antiferromagnetic ordering stability is enhanced by increasing nanoflake size and interaction. In contradistinction to the size dependence of magnetism observed in the zigzag edge structure which is characterized by the shifting of phase transition point in the proximity of zero, the size independent magnetism is found in the armchair edge nanoflakes. These findings thus will contribute to a better understanding of the intrinsic edge magnetism of graphene nanoflakes and enhance its feasibility in spintronic devices. In the

subsequent sections, we in turn suggest research model and method, show results and discussion, and finally give a short conclusion.

2. MODEL AND METHODS

To study the effect of the on-site electron-electron interaction on the magnetic properties in the graphene nanoflakes, we use Hubbard model and its single-band Hamiltonian at half-filling is given as follows:

$$H = -t \sum_{\langle i,j \rangle, \sigma} (a_{i\sigma}^+ b_{j\sigma} + b_{j\sigma}^+ a_{i\sigma}) + U \sum_i (n_{i\uparrow} - \frac{1}{2})(n_{i\downarrow} - \frac{1}{2}). \quad (1)$$

where $a_{i\sigma}^+$ ($b_{i\sigma}$) and $n_{i\sigma} = a_{i\sigma}^+ a_{i\sigma}$ ($n_{i\sigma} = b_{i\sigma}^+ b_{i\sigma}$) are creation (annihilation) and spin density operators at site i for spin σ on sublattice A (B), respectively. t describes the nearest neighbor hopping parameter and the on-site Hubbard interaction is characterized by U . The entanglement of the interaction problem in equation (1) is here addressed within the mean-field theory (MFT). Whereas, the spin density operator $n_{i\sigma}$ is analyzed into an average value plus a small deviation:

$$\begin{aligned} n_{i\uparrow} &= \langle n_{i\uparrow} \rangle + \delta_{i\uparrow}, \\ n_{i\downarrow} &= \langle n_{i\downarrow} \rangle + \delta_{i\downarrow}. \end{aligned} \quad (2)$$

After several simple mathematical calculations, one gets:

$$n_{i\uparrow} n_{i\downarrow} = \langle n_{i\downarrow} \rangle n_{i\uparrow} + \langle n_{i\uparrow} \rangle n_{i\downarrow} - \langle n_{i\uparrow} \rangle \langle n_{i\downarrow} \rangle + \delta_{i\uparrow} \delta_{i\downarrow}. \quad (3)$$

Neglecting a tiny correlation fluctuation $\delta_{i\sigma} \delta_{i\sigma}$, Eq. (1) within the MFT approximation reads

$$\begin{aligned} H^{MF} &= -t \sum_{\langle i,j \rangle, \sigma} (a_{i\sigma}^+ b_{j\sigma} + b_{j\sigma}^+ a_{i\sigma}) \\ &+ U \sum_i (\langle n_{i\downarrow} \rangle n_{i\uparrow} + \langle n_{i\uparrow} \rangle n_{i\downarrow} - \langle n_{i\uparrow} \rangle \langle n_{i\downarrow} \rangle - \frac{1}{2}(n_{i\uparrow} + n_{i\downarrow}) - \frac{1}{4}). \end{aligned} \quad (4)$$

The problem in the Hubbard Hamiltonian is solved by self-consistent algorithm, starting by providing randomly initial values for $\langle n_{i\sigma} \rangle$. The initial values are plugged in the Hubbard Hamiltonian matrix and the iterative calculation is started. At each cycle, the Hamiltonian matrix is diagonalized to get eigenvalues and eigenvectors which are used to compute new spin densities $\langle n_{i\uparrow} \rangle$ and $\langle n_{i\downarrow} \rangle$. These new spin densities are then used as the initial values for the next iteration. The procedure is repeated until satisfying the convergence condition of self-consistency. Eventually, the magnetic moment at site i is computed by the equation:

$$m_i = \frac{\langle n_{i\uparrow} \rangle - \langle n_{i\downarrow} \rangle}{2} \quad (5)$$

The total spin is the sum of $m_i, S = \sum_i m_i$. As a noticeable point, the total spin should be zero for the system with sublattice balance and nonzero for one with sublattice imbalance according to Lieb's theorem.

3. RESULTS AND DISCUSSION

We first revisit the magnetic properties in the infinite graphene system. A Mott-Hubbard point (or a critical point) at $U_c \approx 2.23t$ where the graphene undergoes a phase transition from the

gapless semi-metal to antiferromagnetically ordering insulator is observed. In fact, no accurate value of U_c has been reported due to the absence of direct experimental measurements for the graphene case. Therefore, different numerical approximation results in a variation of U_c , as reported in our previous work [17]. A finite single-particle gap is opened as $U_c > 2.23t$ and is proportional to U and magnetization (see Figure 2).

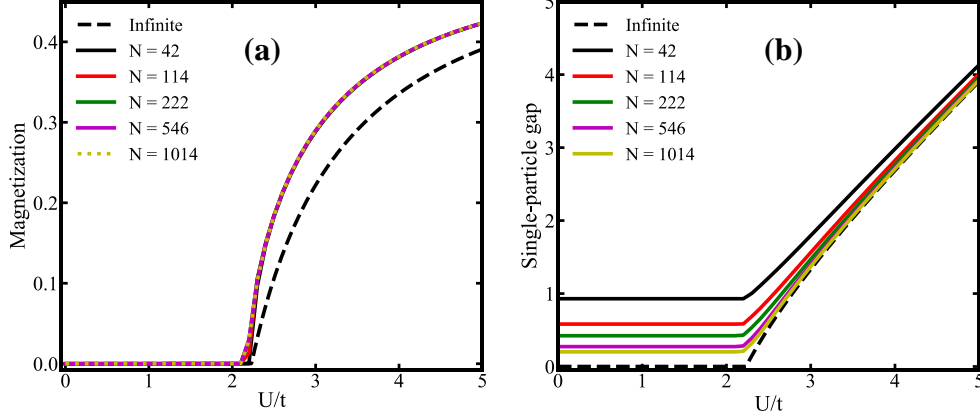


Figure 2. (a) Edge magnetization and (b) single-particle gap of diamond graphene nanoflakes with the armchair edges for different sizes as a function of U/t .

In what follows, we discuss in detail the magnetization on the diamond graphene nanoflakes. Figures 2 and 3 depict the dependence of edge staggered magnetization,

$$M_s = \frac{1}{N_{edge}} \sum_i (-1)^i m_i,$$

where N_{edge} is the number of carbon atoms located at the edges, and single-particle gap on size and Coulomb energy U/t . Dissimilar to the infinite system, there exists a natural band gap in the nanoflakes without interaction and it decreases gradually via the number of sites. A transition from the nonmagnetic to antiferromagnetic states at a finite U , thereafter named U_c , is also observed over all nanoflakes considered. At a weak Coulomb energy U , our calculations show that the spin magnetic moments arrange parallelly along the zigzag edges caused by the edge localized electronic states while such behavior is not formed at the armchair edges where electronic states are delocalized. As shown in Figure 2, due to the symmetry in the sublattices, and the non-existence of zigzag termination, in resemblance to the honeycomb lattice the critical point in the armchair nanoflakes is independent of the number of sites, $U_c \sim 2.23t$. As a consequence, the onset of an antiferromagnetic ordering state appears above the Mott-Hubbard point. These results are in good agreement with previous articles [18]. For the zigzag edge nanoflakes, our calculating results reveal the instability of U_c against the size. In parallel with the decline of the single-particle gap, the U_c is required much lower than $2.23t$ and decreases rapidly upon the size from 30 ($U_c \simeq 1.51t$) to 126 ($U_c \sim 0.01t$) carbon atoms.

With further increasing the size, a tiny value of U_c is needed to enable the spin polarization state, as shown in the inset of Figure 3. The reduction of U_c was reported in hexagon-shaped zigzag graphene nanoflakes within dynamical mean-field theory approximation, typically the U_c

shifts from approximately $3.1t$ ($N = 54$) to $2.0t$ ($N = 150$) [16]. The origination of this phenomenon can be in robust relation to single-particle gap. Figure 3 (b) indicates the inversely proportional single-particle gap to the increase of the size.

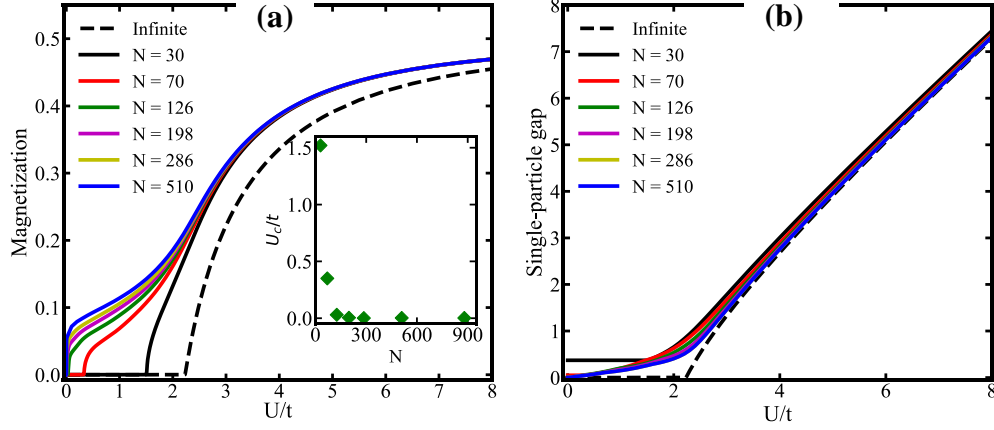


Figure 3. (a) Edge magnetization and (b) single-particle gap of diamond graphene nanoflakes with zigzag edges for different sizes from 30 to 510 carbon atoms as a function of U/t . The inset of (a) denotes the size dependent U_c .

In addition, the magnetic ordering state only occurs at the zigzag termination while the armchair one suppresses the magnetic ordering formation. Consequently, armchair bond density, defined as $\rho = N_{arm}/N_t$ with N_{arm} (N_t) being the number of the armchair bonds (total bonds), contributes considerably to the shift in the transition point U_c . The increase of the number of atoms on the zigzag edges at bigger nanoflakes, while N_{arm} does not change, gives rise to the significant reduction of the armchair bond density, thus leading to favoring antiferromagnetic ordering in larger nanoflakes rather than in smaller ones at weak interactions.

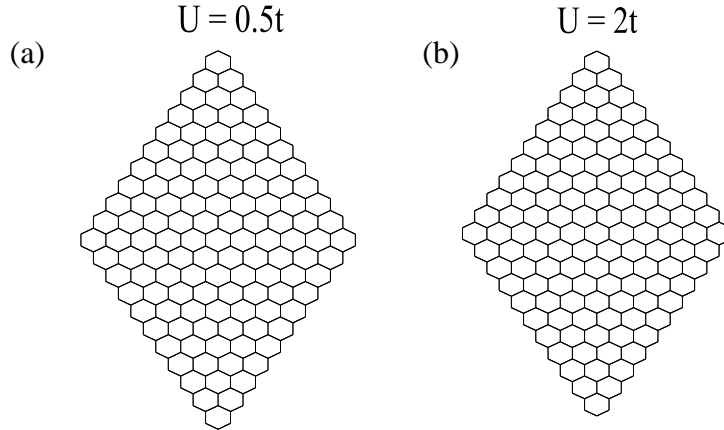


Figure 4. The distribution of local spin moments at each site in $N = 286$ for (a) $U = 0.5t$ and (b) $U = 2t$. The area of each circle denotes the spin moment magnitude at each site.

In the antiferromagnetic state, magnetization increases with the broadening of graphene nanoflakes for $U < 2.23t$. In addition to moving to higher values of both magnetization and gap, their size dependence is negligible as U/t goes far from $2.23t$. At the mean-field level, temporal

fluctuations are not considered, giving rise to overestimate the value of single-particle gap [17]. More remarkably, for a weak U , the spin moments are polarized at the zigzag edge atoms and the magnetization sharply decreases as moving toward the center atoms, typically $U = 0.5t$ (see Figure 4). The spin polarization would occur at all sites with sufficiently strong on-site electron-electron interactions, i.e. $U > 2.23t$. Nevertheless, the local magnetic moments at the edge sites is substantially higher than those of others due to the reduction of the number of hopping channels for the edge sites in comparison with the inner sites. It can be hence confirmed that the primary contribution to the magnetization in the nanoflakes comes from the edge atoms. Moreover, the spin moments on all sites at a given edge align ferromagnetically because all the carbon atoms belong to the same graphene sublattice and such behavior is observed at adjacent edge connected by a zigzag bond. Conversely, the antiferromagnetic alignment at the edge connected by an armchair bond is shown due to atoms belonging to the remaining sublattice. The net total magnetic moment S equals zero, in accordance with Lieb's theorem because the number of atoms in sublattice A is equal to that in sublattice B. Furthermore, it can be obviously seen that since there exists an armchair bond at the junction of the edges the local magnetic moment increases far away from the armchair defect and concurrently is completely suppressed at the armchair defect. As a consequence, the maximum value of local magnetic moment dwells in the edge sites close to the corners for the diamond nanoflakes. The consequence of such a spin distribution is closely related to the distribution of electrons along the edges, as discussed in Ref. [19].

4. CONCLUSIONS

We have produced the first report on how magnetism behaves in a variety of graphene nanoflakes shaped diamonds using the mean-field Hubbard approach. The absence of on-site electron-electron interaction results in a non-magnetic state with all sizes and edge terminations. An antiferromagnetic ground state along the zigzag edges is triggered at a weak interaction U . The spins on the same sublattices exhibit ferromagnetic ordering, while the spins on different sublattices are found to show antiferromagnetic ordering. We found that the magnetization manipulated by the nanoflakes size is a lot more than just due to the Coulomb interaction U . A quite large diamond zigzag nanoflakes require a tiny U_c , leading to the feasible existence of spontaneous magnetization in pure nanostructured graphene. The results are to further enhance the practical possibility of graphene in spintronic applications. m

Acknowledgements. This work was financially supported by the Postdoc Project of the Graduate University of Science and Technology - VAST, Grant code: GUST.STS.ĐT2020–KHV L09. The authors would also like to thank the Institute of Materials Science - VAST for facility supports.

CRedit authorship contribution statement. Phung Thi Thu, Nguyen Thanh Tung: Methodology, Investigation, Funding acquisition and Formal analysis. Nguyen Thi Mai: Investigation, Formal analysis. Pham Thi lien: Formal analysis.

Declaration of competing interest. The authors declare that they have no known competing financial interests or personal relationships that could have appeared to influence the work reported in this paper.

REFERENCES

1. Hu G. and Xiang B. - Recent advances in two-dimensional spintronics, *Nanoscale Res. Lett.* **15** (2020) 226. [https://doi: 10.1186/s11671-020-03458-y](https://doi.org/10.1186/s11671-020-03458-y).

2. Liu Y., Zeng C., Zhong J., Ding J., Wang Z. M., and Liu Z. - Spintronics in two-dimensional materials, *Nano-Micro Lett.* **12** (2020) 93. <https://doi.org/10.1007/s40820-020-00424-2>.
3. Castro Neto A. H., Guinea F., Peres N. M. R., Novoselov K. S., and Geim A. K. - The electronic properties of graphene, *Rev. Mod. Phys.* **81** (1) (2009) 109. <https://doi.org/10.1103/RevModPhys.81.109>.
4. Wakabayashi K., Sasaki K. I., Nakanishi T., and Enoki T. - Electronic states of graphene nanoribbons and analytical solutions, *Sci. Technol. Adv. Mater.* **11** (2010) 054504. <https://doi.org/10.1088/1468-6996/11/5/054504>.
5. Bullock C. J. and Bussy C. - Biocompatibility considerations in the design of graphene biomedical materials, *Adv. Mater. Interfaces* (2019)1900229 (1-15). <https://doi.org/10.1002/admi.201900229>.
6. Roche A. and Valenzuela S. O. - Graphene spintronics: puzzing controversies and challenges for spin manipulation, *J. Phys. D: Appl. Phys.* **47** (9) (2014) 094011. <http://dx.doi.org/10.1088/0022-3727/47/9/094011>.
7. Guimaraes M. H. D., Zomer P. J., Ingla-Aynes J., Brant J. C., and van Wees B. J. - Controlling spin relaxation in hexagonal BN-encapsulated graphene with a transverse electric field, *Phys. Rev. Lett.* **113** (2014) 086602. <https://doi.org/10.1103/PhysRevLett.113.086602>.
8. Dankert A., Kamalakar M. V., Bergsten J., and Dash S. P. - Spin transport and precession in graphene measured by nonlocal and three-terminal methods, *Appl. Phys. Lett.* **104** (2014) 192403. <https://doi.org/10.1063/1.4876060>.
9. Drogeler M., Volmer F., Wolter M., Terres B., Watanabe K., Taniguchi T., Guntherodt G., Stampfer C., and Beschoten B. - Nanosecond spin lifetimes in single- and few-layer graphene-hBN heterostructures at room temperature, *Nano Letts.* **14** (11) (2014) 6050. <https://doi.org/10.1021/nl501278c>.
10. Yazyev O. V. and Helm L. - Defect-induced magnetism in graphene, *Phys. Rev. B* **75** (2007) 125408. <https://doi.org/10.1103/PhysRevB.75.125408>.
11. Wang W., Huang Y., Song Y., Zhang X., Ma Y., Liang J., and Chen Y. - Room-temperature ferromagnetism of graphene, *Nano Lett.* **9** (1) (2009) 220. <https://doi.org/10.1021/nl802810g>.
12. Nair R. R., Tsai I.-L., Sepioni M., Lehtinen O., Keinonen J., Krasheninnikov A. V., Castro Neto A. H., Katsnelson M. I., Geim A. K., and Grigorieva I. V. - Dual origin of defect magnetism in graphene and its reversible switching by molecular doping, *Nat. Commun.* **4** (2013) 2010. <https://doi.org/10.1038/ncomms3010>.
13. Miao Q., Wang L., Liu Z., Wei B., Xu F., and Fei W. - Magnetic properties of N-doped graphene with high Curie temperature, *Sci. Rep.* **6** (2016) 21832. <https://doi.org/10.1038/srep21832>.
14. Blonski P., Tucek J., Sofer Z., Mazanek V., Petr M., Pumera M., Otyepka M., and Zboril R. - Doping with graphitic Nitrogen triggers ferromagnetism in graphene. *J. Am. Chem. Soc.* **139** (8) (2017) 3171. <https://doi.org/10.1021/jacs.6b12934>.
15. Magda G. Z., Jin X. Z., Hagymási I., Vancsó P., Osváth Z., Nemes-Incze P., Hwang C., Biro L. P., and Tapasztó L. - Room-temperature magnetic order on zigzag edges of narrow graphene nanoribbons, *Nature* **514** (2014) 608. <https://doi.org/10.1038/nature13831>.

16. Valli A., Amaricci A., Brosco V., and Capone M. - Quantum interference assisted spin filtering in graphene nanoflakes. *Nano Lett.* **18** (3) (2018) 2158. <https://doi.org/10.1021/acs.nanolett.8b00453>.
17. Raczkowski M., Peters R., Phung T. T., Takemori N., Assaad F. F., Honecker A., and Vahedi J. - Hubbard model on the honeycomb lattice: from static and dynamical mean-field theories to lattice quantum Monte Carlo simulation, *Phys. Rev. B* **101** (2020) 125103. <https://doi.org/10.1103/PhysRevB.101.125103>.
18. Viana-Gomes J., Pereira V. M. and Peres N. M. R. - Magnetism in strained graphene dots, *Phys. Rev. B* **80** (2009) 245436. <https://doi.org/10.1103/PhysRevB.80.245436>.
19. Zarenia M., Chaves A., Farias G. A., and Peeters F. M. - Energy levels of triangular and hexagonal graphene quantum dots: a comparative study between the tight-binding and the Dirac approach. *Phys. Rev. B* **84** (2011) 245403. <https://doi.org/10.1103/PhysRevB.84.245403>.